Electronic Supporting Information for,

Visible light enhanced catalytic activity of Au_n subnanoclusters: the importance of d-sp interband transitions

Alba Sorroche,[a] Irene del-Campo,[a] Alberto Casu,[b] Andrea Falqui,[b] Miguel Monge*[a] and José M. López-de-Luzuriaga*[a]

[a]Departamento de Química, Instituto de Investigación en Química (IQUR). Universidad de La Rioja. Complejo Científico-Tecnológico, 26006 Logroño (Spain).

E-mail: miguel.monge@unirioja.es, josemaria.lopez@unirioja.es

[b]CIMAINA and Departimento di Fisica, Università degli Studi di Milano, Via Celoria 16, 20133 Milano, Italy.

I. Instrumentation/General procedures

Synthesis of Au@PEG: In a 100mL flask equipped with a magnetic stir bar 2 g of polyethyleneglycol was dissolved in 20 mL of methanol. The mixture was stirred at 65 °C until the complete dissolution of the solid and then 0.01 g of AuCl was added allowing the mixture to react for one hour. The reaction was concentrated under reduced pressure to give the product Au@PEG.

In a typical experiment 0.2 g of Au@PEG was placed in a Schlenk flask equipped with a magnetic stir bar. 2 mL of methanol, 100 µL of water and 16 µL of 4-pentynylbenzene were subsequently. The resulting mixture was magnetically stirred at 60 °C.

White and UV LED studies were conducted in an APRIA Systems LED photoreactor equipped with a collimated visible LED lamp.

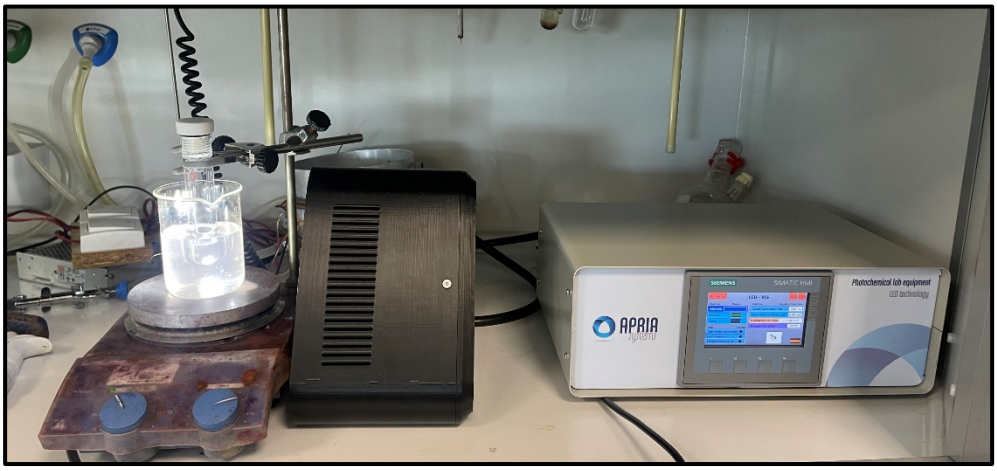

Fig. S1. Apria Systems for White LED light irradiation.

Blue and green light catalytic reactions were conducted using a lab-made assembly consisting of four 10 W blue/green light LED lamps (LED-Engin, CA, USA). These lamps were placed equidistantly inside an 18-cm cylinder with circulating cooling water to regulate the glass reactor at a constant temperature of 25 °C.

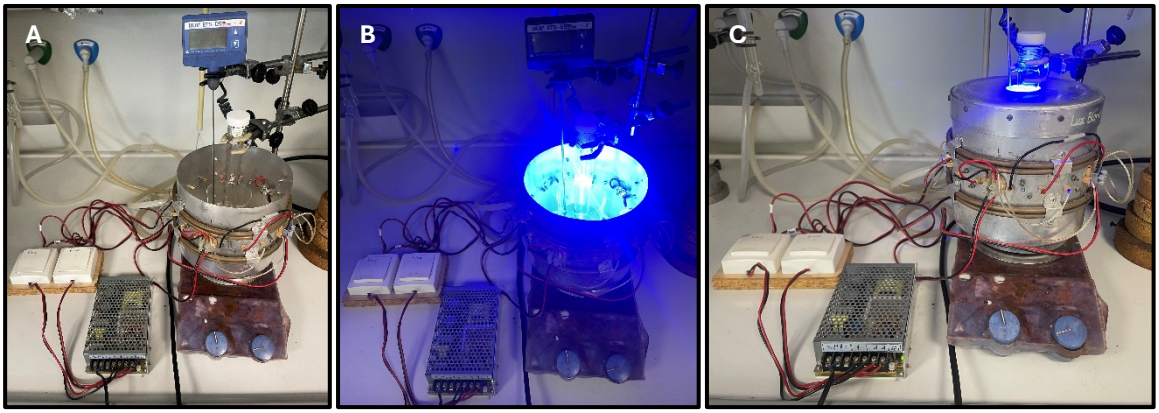

Fig. S2. Home made irradiation setup for blue and green light irradiation.

The presence of subnanoclusters was analyze by taken a sample by each time of the reaction for MALDI-TOF analysis. MALDI-TOF spectra were recorded in a Microflex MALDI-TOF Bruker spectrometer. The samples were prepared by adding 1 µL of the reaction mixture on a hole of a MSP ground Steel BC sample holder (Bruker). The samples were dried before the measurements.

The quantitative monitoring of the catalytic reaction was performed by gas chromatography using a Agilent 8890 GC System, equipped with a J&W HP-5ms Ultra Inert GC Column (30 m x 0.25 mm x 0.25 µm) and MS detector (electron impact with a single quadrupole filter). A split injection system with a split ratio of 100:1 was used with helium as carrier gas at head pressure of 10.4 psi. The temperature programming was 40 °C/min, 180 °C (3min) and 60°C/min (5min), 300°C (7 min). The conversion of the alkyne reactive and the ketone product yield were analyzed by integrating the chromatographic peaks of 4-pentynylbenzene (retention time 3.165 min) and 5-phenylpentan-2-one (retention time 3.750 min).

UV/Vis/NIR spectra were recorded with a Shimadzu UV-3600 UV-Vis-NIR spectrophotometer.

II. **Characterization data**

a. **MALDI**

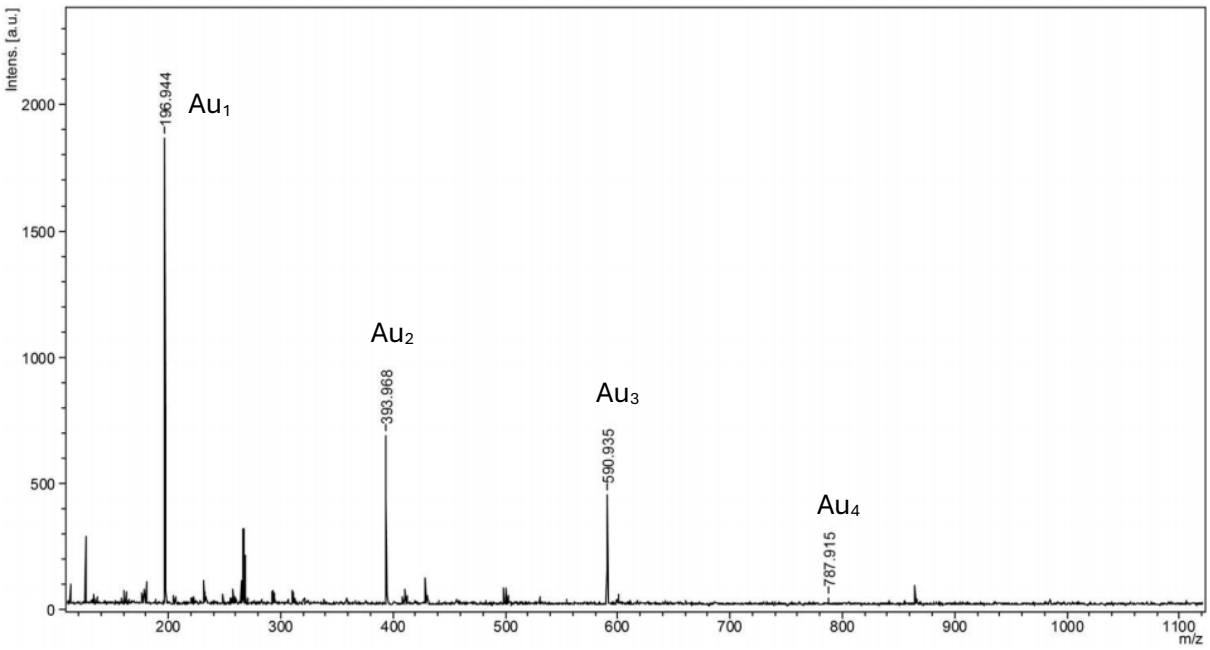

Fig. S3. MALDI-TOF in its negative mode showing the formation of small gold clusters inside of a polyethylene glycol matrix.

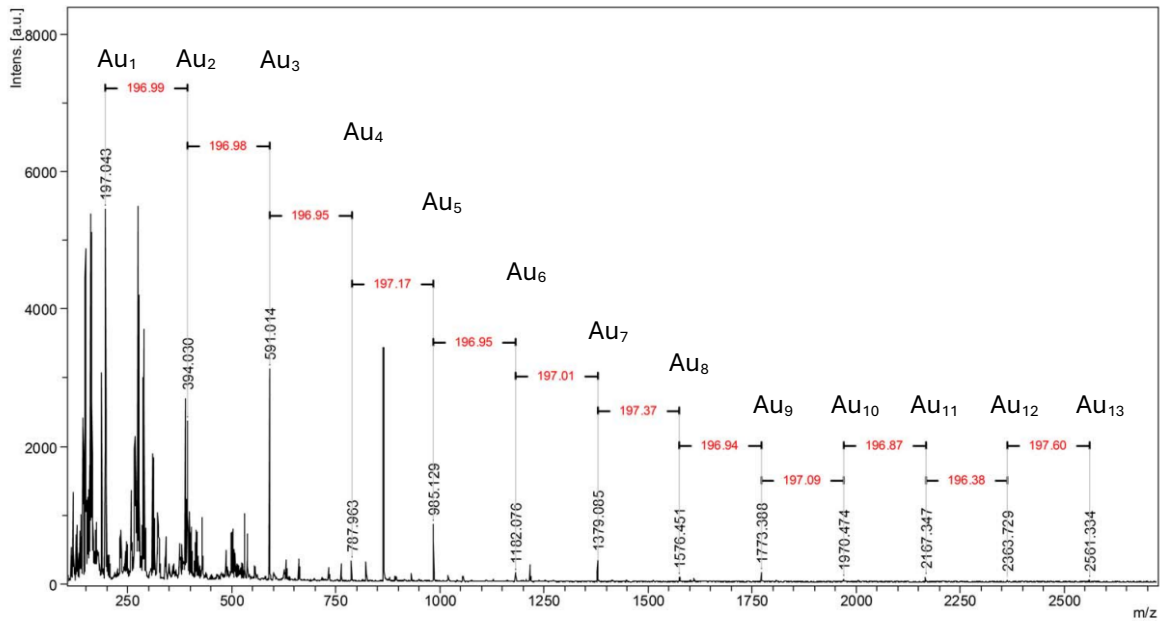

Fig. S4. MALDI-TOF in its negative mode showing the formation of larger size gold clusters at 30 minutes of reaction conditions. No stabilizer agent was used. (AuCl in MeOH)

The MALDI spectrum registered before light irradiation shows the presence of very small Au_n species already present in the catalyst (14% of Au SNCs detected in the XPS spectrum). However, the amount of these catalytic species is appreciably less under dark conditions than those obtained when we activate the catalyst with light (Fig S5). Indeed, when the catalyst is used under dark conditions a much lesser catalytic activity is detected (see Figure S10).

Moreover, addition of the alkyne to the Au@PEG solution together with 30 minutes of irradiation reveal peaks up to seven gold atoms (1378,4 m/z). The addition of the alkyne results in a purple coloration in the solid, likely caused by the aggregation of gold SNCs into NPs during the reaction. However, the spectrum in Figure S6 indicates that Au SNCs are still present after the addition of the alkyne and after 30 minutes of reaction, due to the continuous generation of these species through the detachment of Au SNCs from Au NPs when irradiated. It is also important to highlight that Au NPs are not catalysts for the hydration of alkynes since it is not possible to activate the alkynes through a π-interaction.[1]

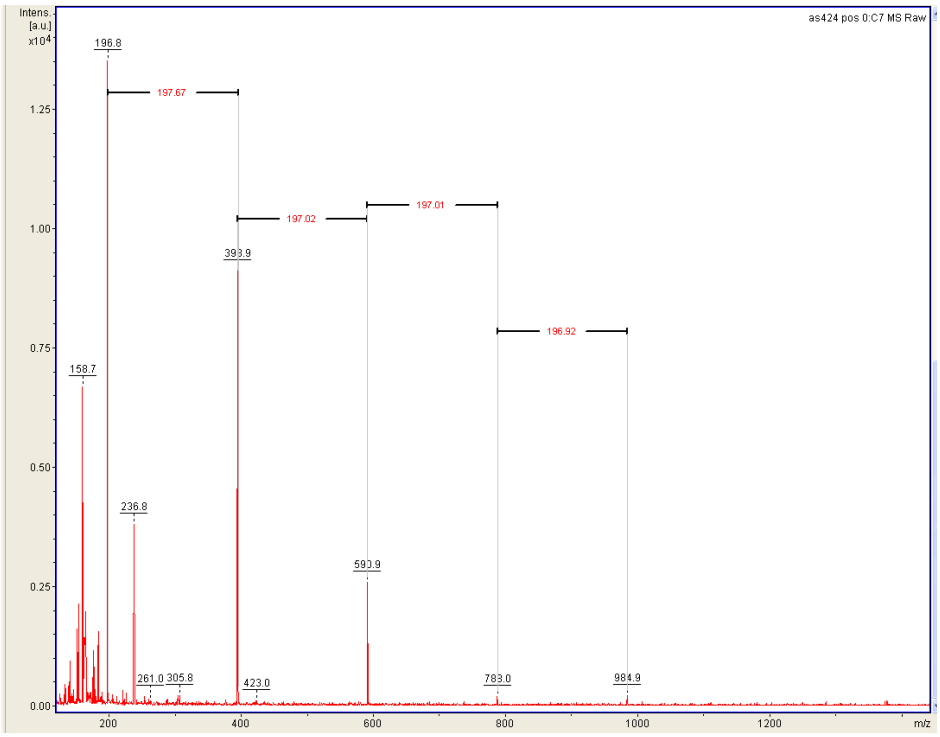

Fig. S5. MALDI spectrum of Au@PEG after 30 minutes of white LED light irradiation.

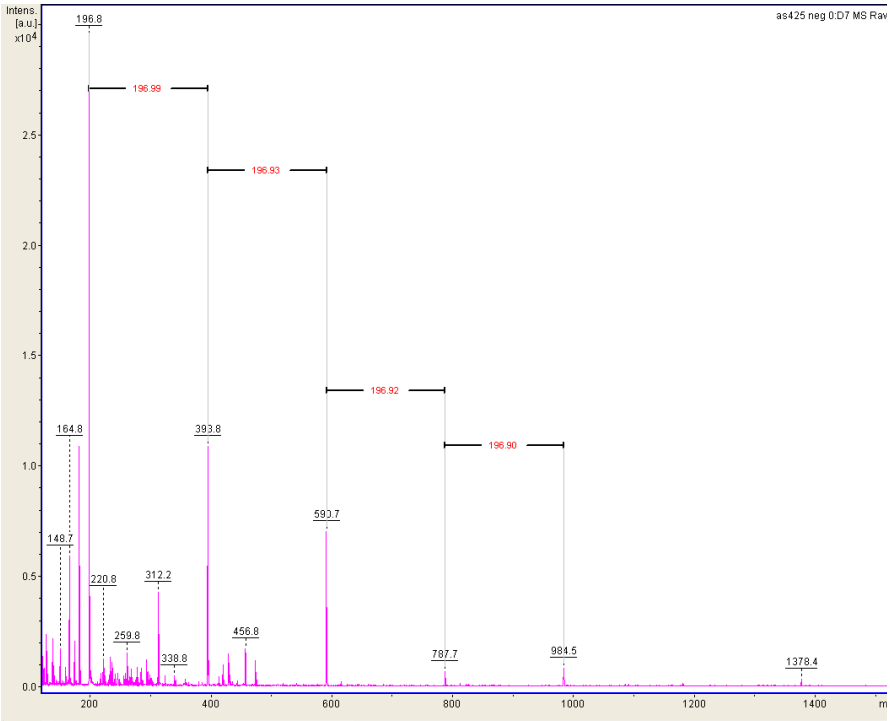

Fig. S6. MALDI spectrum of Au@PEG with the addition of the alkyne after 30 minutes of white LED light irradiation.

b. **XPS**

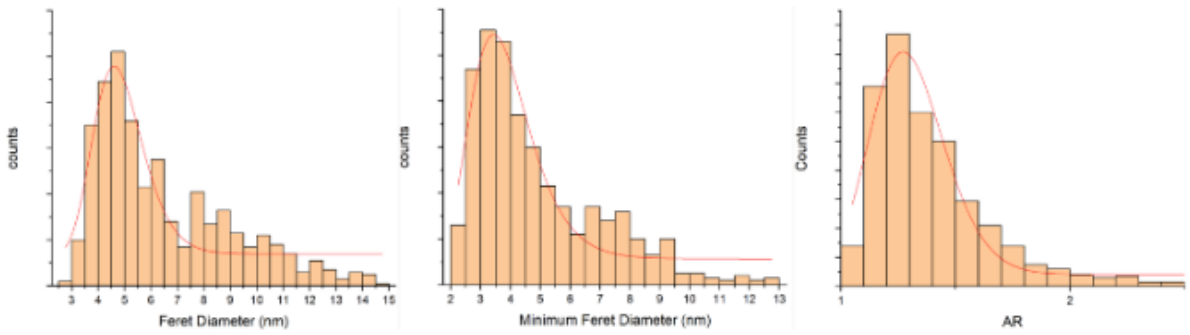

Fig. S7. Size analysis histograms for PEG-Au-NPs.

c. **UV-Vis**

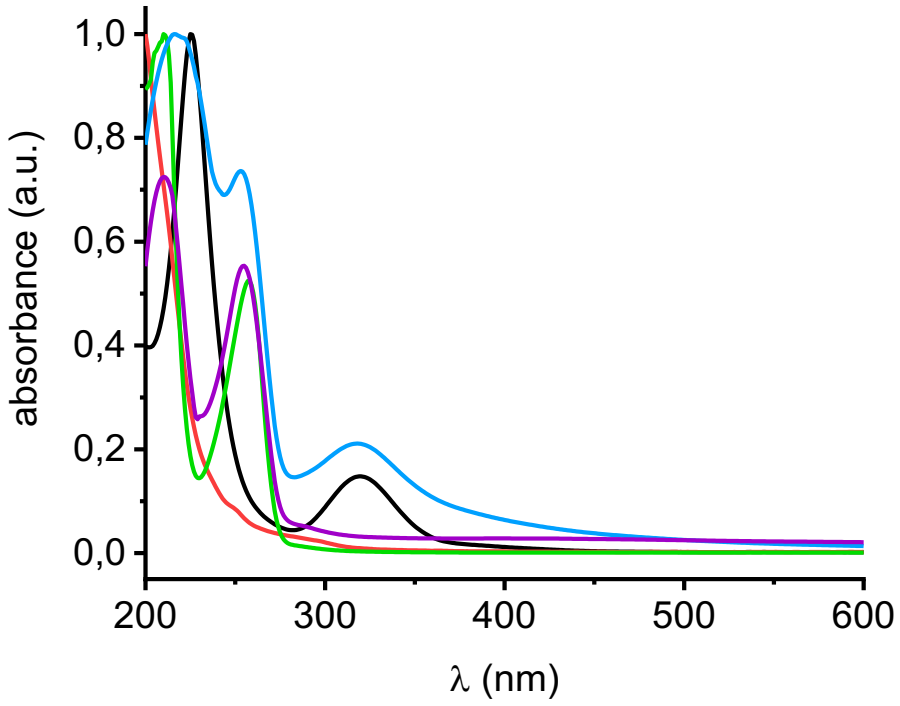

Fig. S8. UV/Vis spectra of a solution of polyethyleneglycol (red); 5-phenyl-1-pentyne (green); Au@PEG (**1**) (black); Au@PEG (**1**) + 5-phenyl-1-pentyne (blue) and Au@PEG (**1**) + 5-phenyl-1-pentyne after the catalytic reaction (purple).

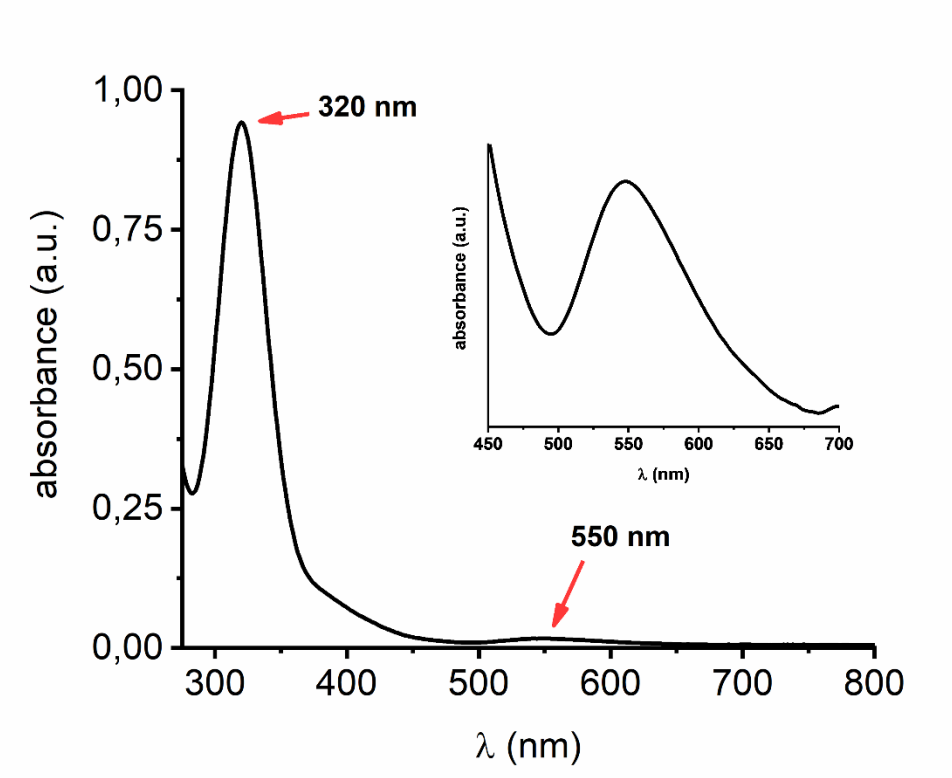

Fig. S9. Enlargement of the UV/Vis spectra of a solution of Au@PEG (**1**).

In the Au@PEG UV-Vis spectrum (Fig.S9), we can see an absorbance peak at 320 nm which could be attributed to Au NCs. There is also a minor absorption peak at 550 nm associated to the typical LSPR absorption of AuNPs. However, significant absorption in the visible region becomes more apparent after the addition of the alkyne (blue line, Fig. S8). In this sense, a previous study reported by our group showed how the stabilization of Au SNCs with different alkynes presents different optical properties such as the luminescence in the visible range. Only Au_n-alkyne species reveal this luminescence while naked Au SNCs do not exhibit emissions in this range.[2]

The addition of the reactants (with a proportion of 4% Au@PEG) initiates the catalytic cycle through Au···π(alkyne) interaction and the absorption of white light. Upon completion of the reaction, the absorption peak at 320 nm disappears and a broad absorption arises around 500 nm (purple line Fig. S8), likely due to the aggregation of the Au SNCs into Au(0) nanoparticles. This observation aligns with the purple colour seen in the solid obtained post-reaction. It is important to note the vanish of the 320 nm peak probably due to the consumption of Au NCs and the decomposition in bulk Au(0).

III. **Catalytic experiments**

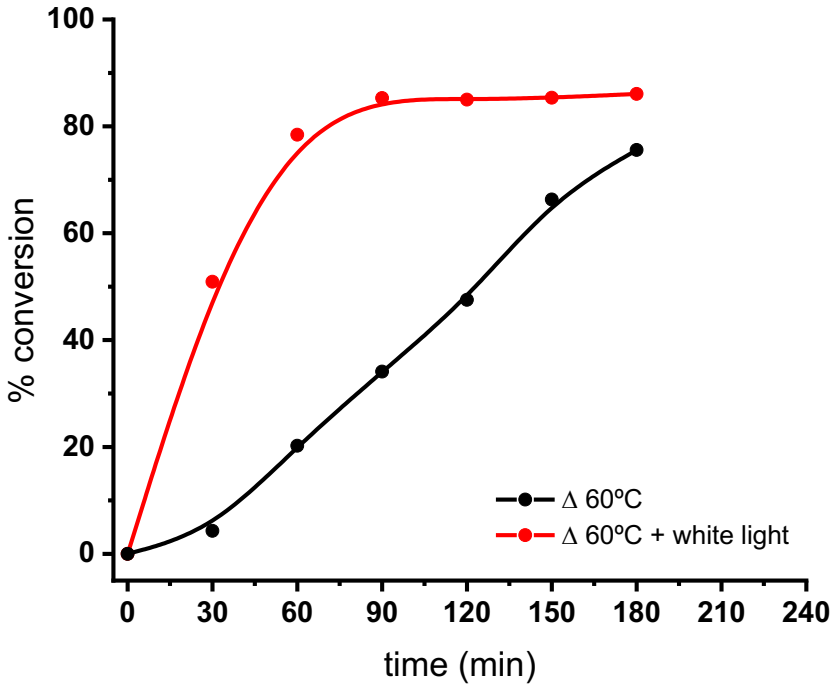

Fig. S10. Hydration of 5-phenyl-1-pentyne catalyzed using Au@PEG (**1**) as catalyst with conditions of 60 °C (black) or 60 °C + white LED irradiation (blue)

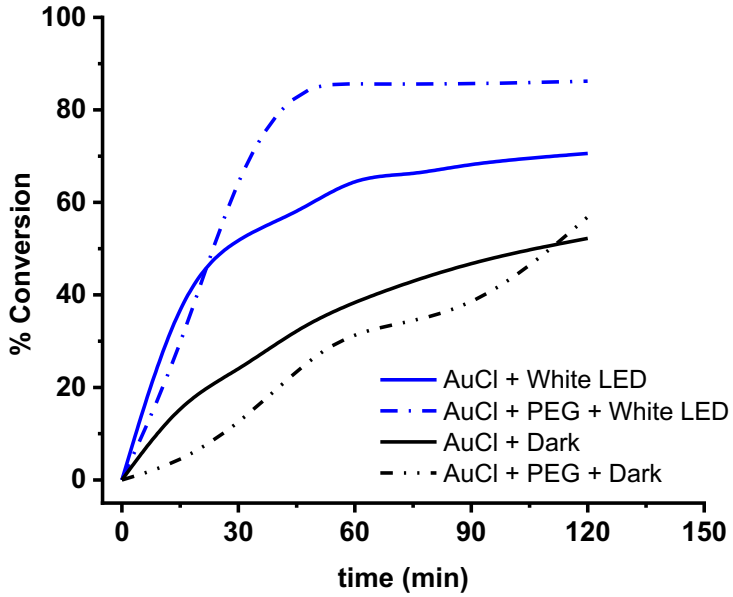

Fig. S11. Kinetics of alkyne hydration at different reaction conditions using 4% AuCl as precatalyst at 60 °C. Conditions used: Dark (black), dark and polymeric environment (dashed black), white LED light (blue) and white LED light and polymeric environment (dashed blue).

In a previous study reported by our group, we demonstrated that gold SNCs were generated from AuCl in the reaction medium (methanol) and that they were useful to catalyse the hydration of alkynes.[7] The reductive medium of the reaction (solvent) is enough to generate SNCs of small sizes (Au_3-Au_5) and thus, it would be interesting to know if we would reach similar results for the same reaction in a polymer matrix.

When using AuCl in a polymeric matrix environment, we observe that AuSNCs and AuNPs are created and stabilized *in situ* in high concentrations thanks to the reductive medium, as it is demonstrated by the catalytic activity in the hydration of 5-phenyl-1-pentyne and observed in the MALDI spectrum (Fig S3). Significantly, the use of white LED light excites the LSPR of the *in situ* formed Au NPs instead of favouring the aggregation of catalytic species, resulting in the creation of more SNCs and an enhanced catalytic efficiency (see Fig S11). This leads to exactly the same situation that we observe when using Au@PEG with 14% of Au SNCs sample as catalyst in this work.

Finally, we compared the hydration of 5-phenyl-1-pentyne using AuCl without a PEG matrix polymer, in the presence and in the absence of light (Fig S11). Importantly, we detect a lower catalytic activity in both cases, what can be explained by a higher aggregation rate of the Au SNCs and Au NPs in the medium, when these are not protected by the PEG matrix.

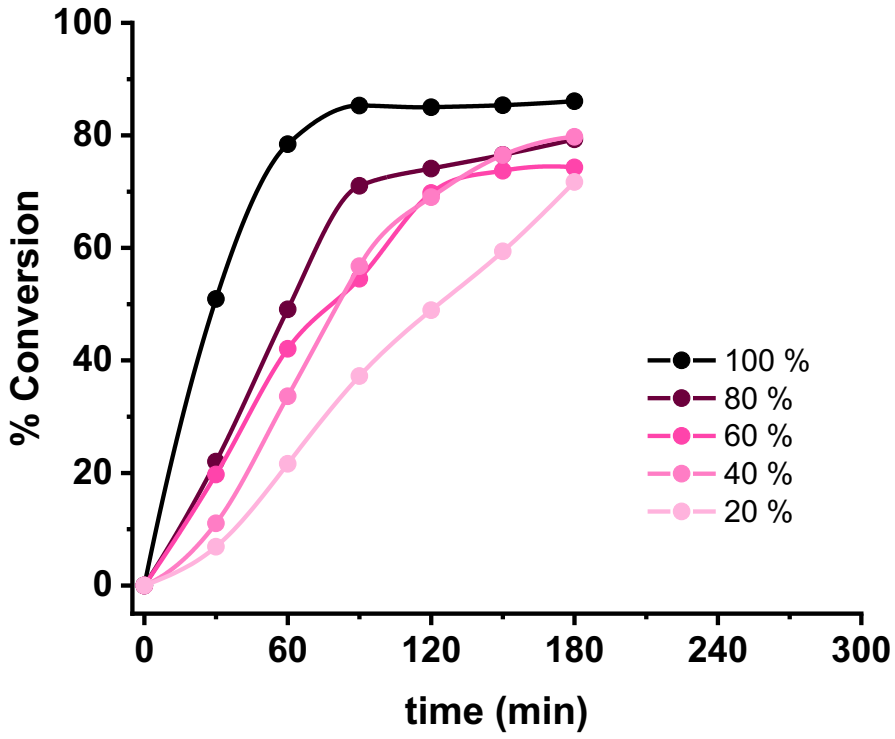

Fig. S12. Kinetics of alkyne hydration at different values of white LED light irradiance.

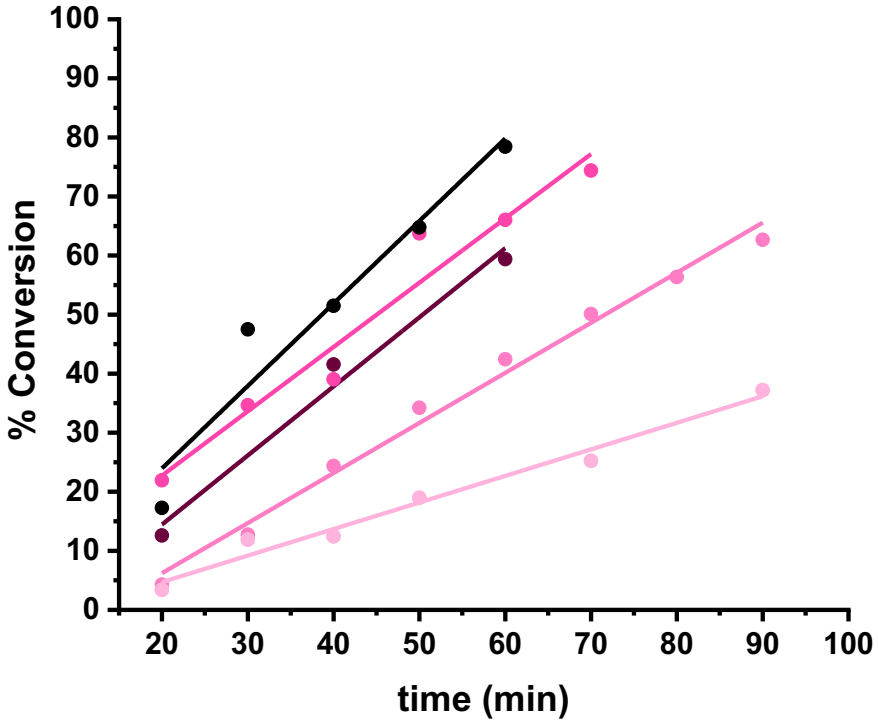

Fig. S13. Kinetics of alkyne hydration at different light irradiance ($W \cdot m^{-2}$) fitted using a linear law.

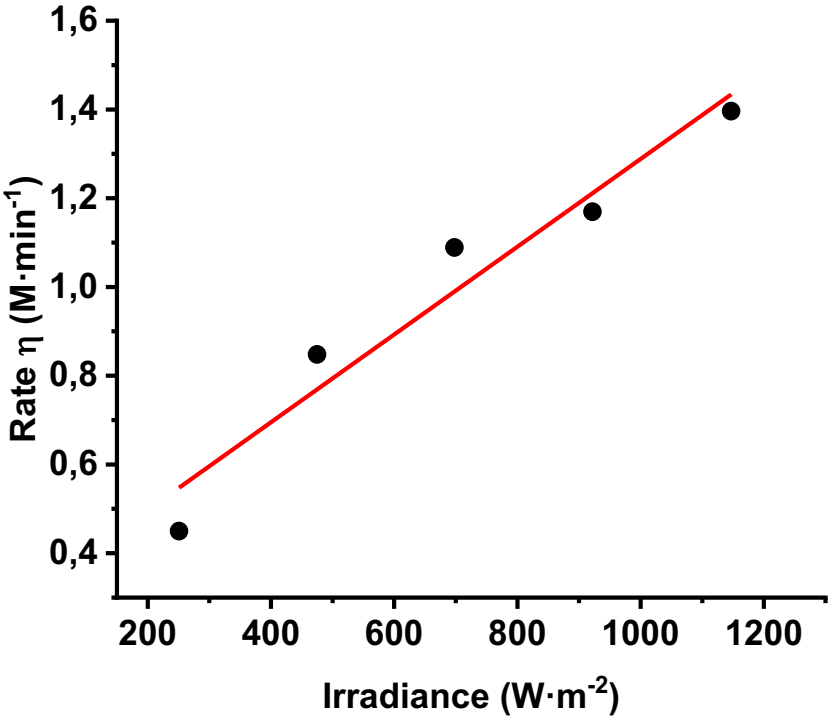

Fig. S14. Chemical rate of alkyne hydration as function of light irradiance ($W \cdot m^{-2}$) fitted using a linear law.

Table S1. Chemical rate of alkyne hydration as function of light irradiance ($W \cdot m^{-2}$).

Irradiance ($W \cdot m^{-2}$)	Slope ($M \cdot min^{-1}$)
0	0.48399±0.0201
251	0.44960±0.03435
475	0.84786±0.03567
698	1.08879±0.1248
922	1.16960±0.16074
1147	1.39615±0.21607

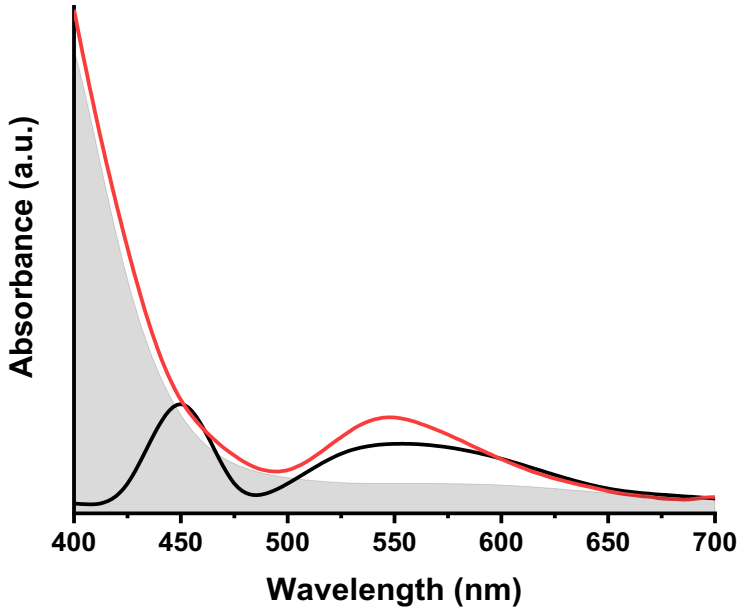

Fig. S15. Simulated UV/Vis spectra of a white LED light absorbance (black) and UV/Vis spectra of Au@PEG (**1**) compound (red).

IV. Computational Methods

DFT/TD_DFT calculations were performed using the ORCA program versions 4.0 [3] and 5.0.[4] using RI-DFT/BP-D3(BJ) level of theory with def2-SVP [5] basis set. the exchange functional according to Becke [6] and the correlation functional suggested by Perdew [7] called BP, with the resolution of the identity (RI) approximation and def2-SVP basis set.

Multiwfn 3.8 tool was used to calculate hole-electron interactions of the more relevant electronic transitions.[8] Chimera is used to visualize some results.[9]

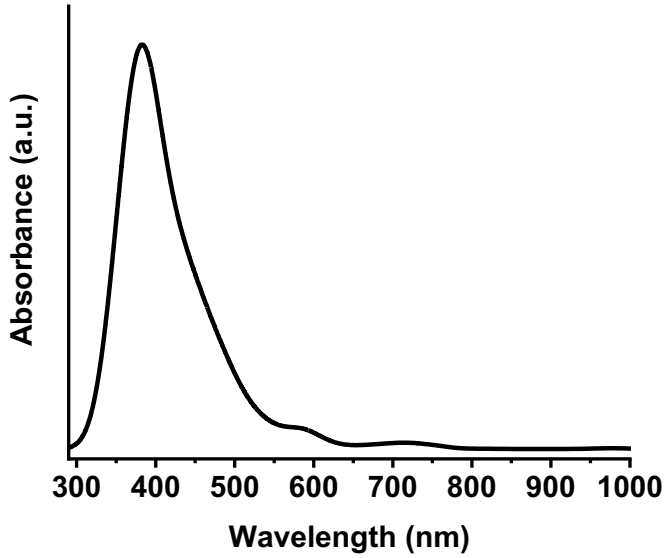

Fig. S16. Theorical absorbance of Au_{13}+ 5-phenyl-1-pentyne (**1a**) model system.

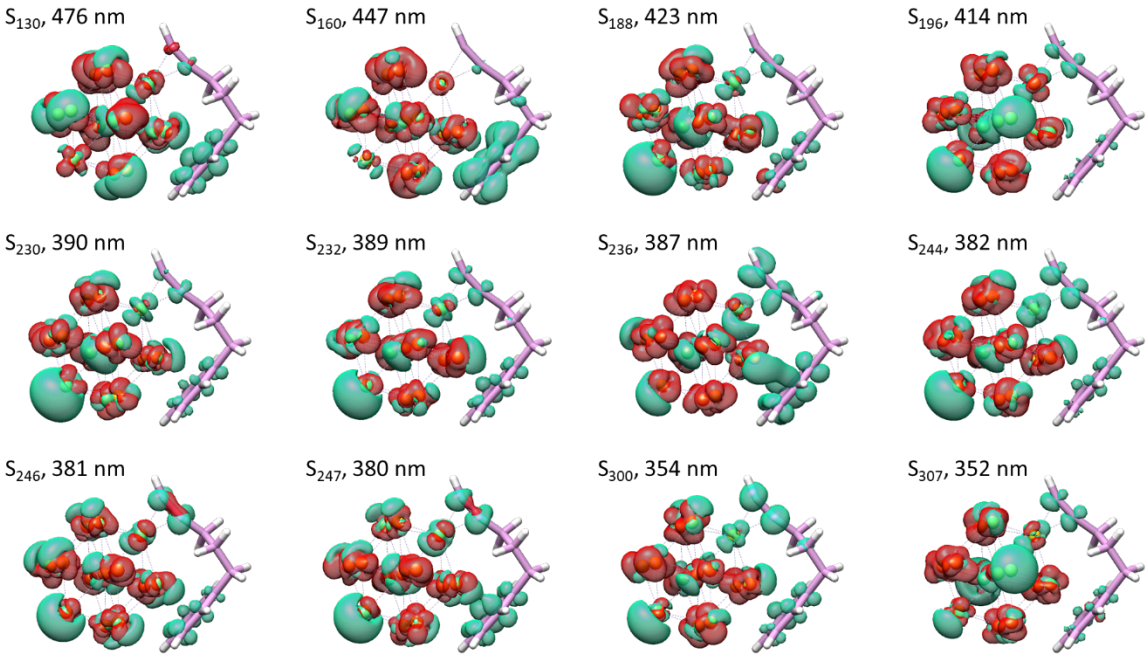

Fig. S17. Representations of electron-hole distribution at different excitations.

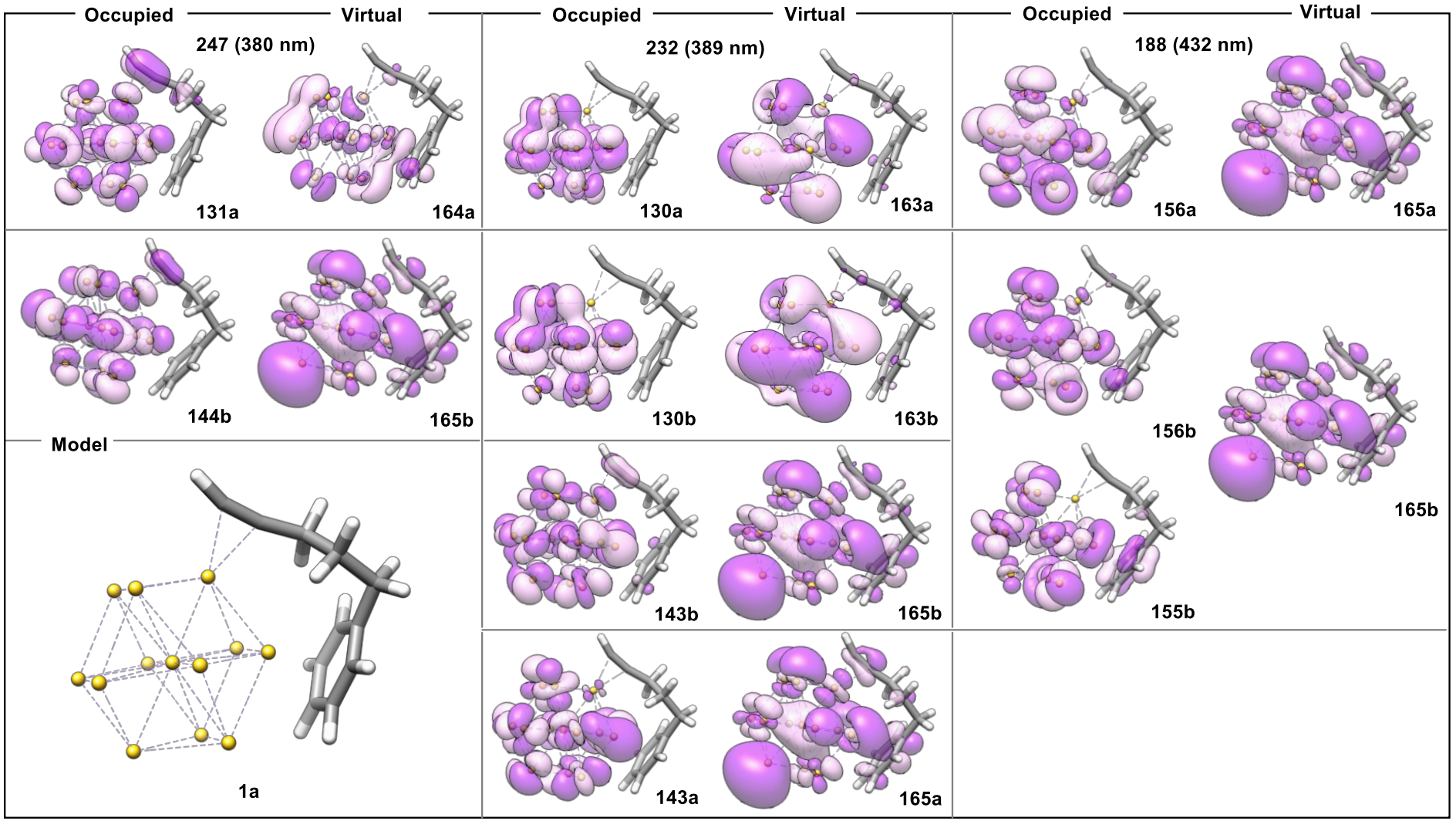

Fig. S18. Molecular orbital plots of different transitions corresponding to three excitations (247, 232 and 188) of **1a** model system.

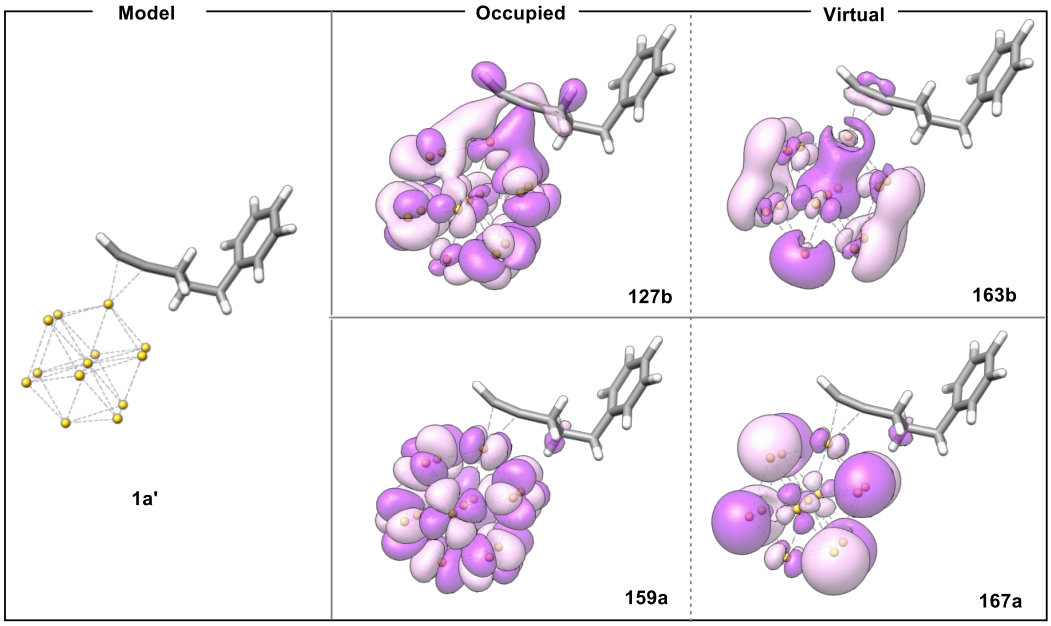

Fig. S19. Molecular orbital plots of transition 247 of the model **1a'** in which the phenyl group is oriented outwards, ruling out the stabilization of the gold nanoparticle.

V. XYZ Coordinates of 1a and 188, 232 and 247 excited states

Au13_pentynyl (1a)

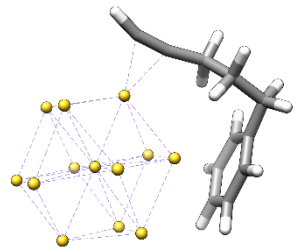

Au	25.054628	24.730697	25.002668
Au	24.669075	22.543858	23.301859
Au	25.134246	23.016960	27.096550
Au	24.890134	26.463004	22.814999
Au	25.459881	26.978038	26.613961
Au	22.747136	24.692043	23.250486
Au	23.200968	25.159940	27.174115
Au	26.804833	24.392583	22.664919
Au	27.348039	24.855088	26.652778
Au	22.764359	22.955663	25.438666
Au	23.146026	26.924526	24.987706
Au	26.988318	22.637341	24.853778
Au	27.234676	26.595353	24.398583
C	25.945047	21.504197	28.525886
C	24.697111	21.576580	28.681781
H	23.696923	21.391511	29.064242
C	27.380564	21.206170	28.554845
H	27.916808	22.178208	28.546949
H	27.621157	20.713011	29.522851
C	27.865130	20.341227	27.372171
H	27.311191	20.650362	26.452726
H	27.610858	19.277263	27.553889
C	29.378927	20.505610	27.104171
H	29.698184	19.719604	26.390059
H	29.949426	20.339464	28.042828
C	29.690386	21.870357	26.533918
C	29.592283	22.090014	25.134567

C 29.961091 22.977082 27.363724

C 29.778565 23.380633 24.582461

H 29.457812 21.227065 24.460955

C 30.092240 24.274991 26.826138

H 30.066765 22.831712 28.449862

C 30.011227 24.479938 25.429819

H 29.738097 23.525066 23.492417

H 30.320971 25.122172 27.490482

H 30.145013 25.485305 25.005594

188

Au 25.071855 24.744880 25.004257

Au 24.697413 22.621207 23.209039

Au 25.096531 22.965008 27.048066

Au 24.941402 26.563709 22.844631

Au 25.441881 26.888540 26.769734

Au 22.793842 24.760417 23.237279

Au 23.169263 25.111650 27.209051

Au 26.852462 24.471877 22.694015

Au 27.355963 24.829709 26.701115

Au 22.747394 22.928137 25.365580

Au 23.177515 26.921644 25.041543

Au 26.972216 22.627940 24.854039

Au 27.248435 26.649961 24.508524

C 25.931924 21.472973 28.541264

C 24.682486 21.538607 28.666630

H 23.673934 21.354864 29.027742

C 27.375379 21.227312 28.568064

H 27.877658 22.217252 28.519090

H 27.641735 20.780434 29.551700

C 27.880915 20.337146 27.412942

H 27.325249 20.607025 26.483610

H 27.647086 19.274567 27.627628

C 29.393122 20.523265 27.149300

H 29.734154 19.718183 26.467063

H 29.957935 20.402734 28.098332

C 29.683536 21.872665 26.533952

C 29.581493 22.046622 25.126249

C 29.938577 23.007082 27.328871

C 29.774607 23.319558 24.533487

H 29.457354 21.161710 24.480678

C 30.050425 24.293319 26.751156

H 30.049792 22.897332 28.418695

C 29.994091 24.447819 25.344546

H 29.750455 23.425927 23.438975

H 30.276747 25.161757 27.388347

H 30.123271 25.439804 24.888208

232

Au 25.080359 24.733475 25.002681

Au 24.669100 22.537261 23.311700

Au 25.067152 23.003588 27.112725

Au 24.937726 26.517652 22.805949

Au 25.496270 26.943886 26.667232

Au 22.777986 24.720594 23.282854

Au 23.161549 25.120101 27.171667

Au 26.824338 24.392862 22.668865

Au 27.339894 24.804720 26.721506

Au 22.733706 22.902789 25.404512

Au 23.198245 26.938889 25.036092

Au 26.980355 22.617843 24.860382

Au 27.285542 26.556909 24.441883

C 25.924050 21.482193 28.535295

C 24.674926 21.534321 28.692423

H 23.678073 21.331643 29.075297

C 27.364677 21.218420 28.556100

H 27.879417 22.202396 28.532172

H 27.625414 20.742099 29.527769

C 27.858749 20.350957 27.379353

H 27.301180 20.645994 26.457183

H 27.615773 19.285756 27.568914

C 29.370551 20.532083 27.113539

H 29.703528 19.738232 26.414353

H 29.937154 20.388386 28.058122

C 29.672644 21.890781 26.524918

C 29.574891 22.092084 25.118836

C 29.937793 23.007288 27.340697

C 29.802350 23.372816 24.551222

H 29.455954 21.219331 24.455340

C 30.077582 24.301445 26.786970

H 30.037963 22.875114 28.429083

C 30.037737 24.479704 25.382992

H 29.781764 23.500056 23.458489

H 30.310913 25.154786 27.441292

H 30.192791 25.476182 24.944996

247

Au 25.079330 24.728130 25.022270

Au 24.708680 22.534547 23.276624

Au 25.046884 22.978014 27.111288

Au 24.983074 26.521966 22.807527

Au 25.447288 26.989514 26.693420

Au 22.823729 24.714248 23.218103

Au 23.179764 25.161561 27.178810

Au 26.856807 24.403440 22.715877

Au 27.305880 24.836733 26.754289

Au 22.731262 22.965989 25.399321

Au 23.219281 26.942215 24.983562

Au 26.967132 22.611556 24.904357

Au 27.261977 26.605710 24.485671

C 25.926472 21.477376 28.521363

C 24.673233 21.509124 28.681828

H 23.692622 21.273714 29.089726

C 27.368797 21.218524 28.554488

H 27.882045 22.203378 28.525892

H 27.626587 20.750777 29.531458

C 27.873009 20.341740 27.388937

H 27.315231 20.624016 26.462226

H 27.636654 19.276696 27.587749

C 29.384302 20.528940 27.122340

H 29.721940 19.731876 26.428938

H 29.951985 20.397216 28.067808

C 29.675865 21.884844 26.523144

C 29.550958 22.080055 25.118968

C 29.960209 23.004595 27.329615

C 29.751946 23.361431 24.543452

H 29.419221 21.205263 24.460608

C 30.086045 24.295061 26.768686

H 30.082584 22.875331 28.416041

C 30.002423 24.472461 25.368483

H 29.710178 23.485295 23.450705

H 30.325444 25.152372 27.415511

H 30.139258 25.468928 24.924317

247 (1a')

Au 25.126798 24.686407 24.424316

Au 24.433217 22.272446 23.155144

Au 24.878032 23.554160 26.917897

Au 25.324845 25.866525 21.860279

Au 25.859827 27.136626 25.637208

Au 22.867807 24.586718 22.598054

Au 23.364627 25.937298 26.340733

Au 26.869065 23.537500 22.362842

Au 27.438339 24.835957 26.158418

Au 22.634910 23.444666 25.157129

Au 23.595639 27.076778 23.767119

Au 26.717668 22.366621 24.973841

Au 27.582957 25.991881 23.618065

C 25.669168 22.554389 28.828285

C 24.427392 22.761390 28.888130

H 23.417769 22.757743 29.294808

C 27.085713 22.250420 29.016596

H 27.176472 21.603353 29.918911

H 27.441028 21.649040 28.149765

C 27.970739 23.498437 29.181886

H 27.581561 24.126137 30.010820

H 27.876439 24.122496 28.247960

C 29.449489 23.147600 29.406541

H 30.025969 24.094395 29.459500

H 29.831043 22.593885 28.522922

C 29.669895 22.330926 30.662495

C 29.547021 22.930660 31.934904

C 29.940607 20.948575 30.595615

C 29.690266 22.169656 33.105934

H 29.339118 24.010653 32.007635

C 30.087395 20.183355 31.765891

H 30.044279 20.466995 29.610048

C 29.960180 20.792486 33.024886

H 29.595285 22.655730 34.089205

H 30.306674 19.107254 31.691963

H 30.076567 20.196938 33.942957

VI. References

1 M. Boronat, A. Leyva-Pérez, A. Corma, *Acc. Chem. Res.* 2014, **47**, 834-844.

2 J. Cordón, G. Jiménez-Osés, J. M. López-De-Luzuriaga, M. Monge, *Nat. Commun.*, 2017, **8**, 1–8.

3 F. Neese, *Wiley Interdiscip. Rev. Comput. Mol. Sci.*, 2018, **8**, 4–9.

4 F. Neese, *Wiley Interdiscip. Rev. Comput. Mol. Sci.*, 2022, **12**, 1–15.

5 F. Weigend and R. Ahlrichs, *Phys. Chem. Chem. Phys.*, 2005, **7**, 3297–3305.

6 A. D. Becke, *Phys. Rev. A (Coll Park)*, 1988, **38**, 3098–3100.

7 J. P. Perdew, *Phys. Rev. B*, 1986, **33**, 8822–8824.

8 T. Lu and F. Chen, *J. Comput. Chem.*, 2012, **33**, 580–592.

9 E. F. Pettersen, T. D. Goddard, C. C. Huang, G. S. Couch, D. M. Greenblatt, E. C. Meng and T. E. Ferrin, *J. Comput. Chem.*, 2004, **25**, 1605–1612.